

First Physics at LHC with ATLAS

Muon trigger efficiency

The Large Hadron Collider

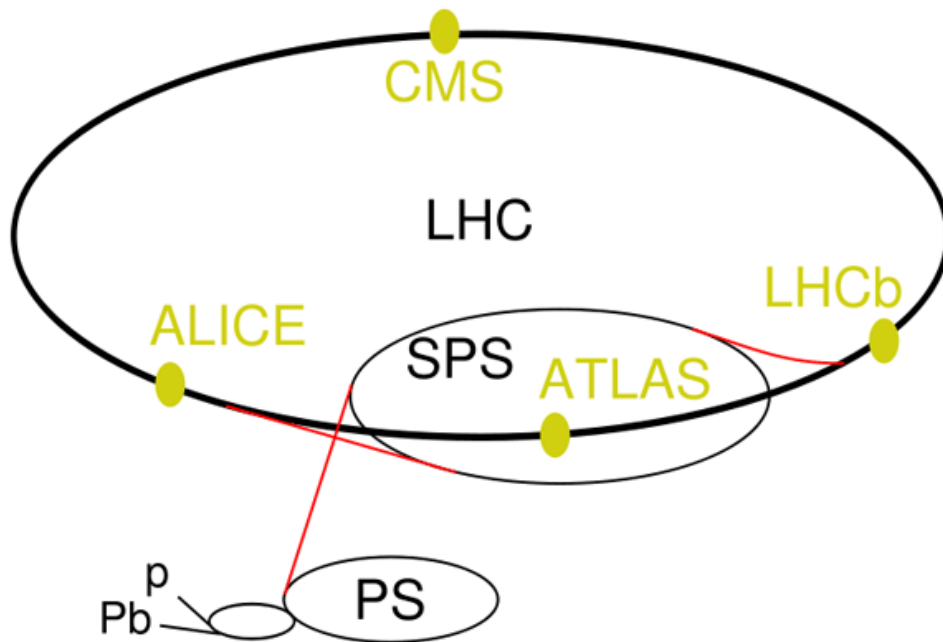


Figure 1: The LHC accelerator chain[7].

The Large Hadron Collider (LHC), is a circular accelerator built at CERN. It is hosted in the former LEP tunnel, and it will accelerate two proton beams in separate rings up to a centre of mass energy of 14 TeV. The machine is also designed to provide heavy ion collisions (Pb-Pb) at an energy of 1150 TeV at the centre of mass, corresponding to 2.76 TeV/nucleon. The design luminosity for pp operation is $10^{34} \text{cm}^{-2} \text{s}^{-1}$, and by modifying the existing antiproton ring (LEAR) into an ion accumulator, the peak luminosity in Pb-Pb operation can reach $10^{27} \text{cm}^{-2} \text{s}^{-1}$. Figure 1. shows a schematic view of the layout of the machine and detectors. The two particle beams cross in four points (thus making their path length identical), which are the four collision points available for experiments. The two high luminosity intersections at points 1 and 5, diametrically opposed, host the experiments ATLAS and CMS respectively. Two more experiments, one aimed at the study of heavy ions collisions (ALICE) and one designed to perform accurate studies of B-physics (LHCb) will be located at point 2 and point 8 [2,8].

p-p operation. The beams in the LHC will contain 2835 bunches of 10^{11} protons each. The existing CERN accelerator chain, illustrated in Figure 1., will be used as an injection system for the LHC.

The bunches, with an energy of 26 GeV are formed in the RFQ/LINAC2 and then are injected into Booster and the PS, and are characterized by a 25ns spacing. Three trains of 81 bunches, corresponding to a total charge of $2.43 \cdot 10^{13}$ protons, are injected into the SPS on three consecutive PS cycles, thus filling 1/3 of the SPS circumference. The resulting beam is accelerated to 450 GeV before being transferred to the LHC. This cycle has to be repeated 12 times in order to fill both of the LHC counter-rotating beams [7].

The ATLAS experiment

ATLAS (A Toroidal Lhc ApparatuS) is one of the four experiments installed at the LHC. One of the main physics issues that will be the centre of mass energy and luminosity of the LHC allow to investigate is the origin of the spontaneous symmetry-breaking mechanism in the electroweak sector of the Standard Model (SM). This symmetry-breaking is expected to cause the existence of a SM Higgs boson, or of a family of Higgs particles if the Minimal Supersymmetric Standard Model (MSSM) is considered. The design of the ATLAS detector was therefore optimized to allow the identification of Higgs particles [8].

Overall design

In order to achieve the necessary sensitivity to the physics processes which are to be studied at the LHC, the ATLAS detector has been designed to provide:

- Electron and photon identification and measurements, using a very precise electromagnetic calorimetry.
- Accurate jet and missing transverse momentum measurements, using, in addition to electromagnetic calorimeters, the full-coverage hadronic calorimetry.
- Efficient tracking also at high luminosity, with particular focus on high-pT lepton momentum measurements.
- Large acceptance in pseudorapidity, and almost full coverage in ϕ .

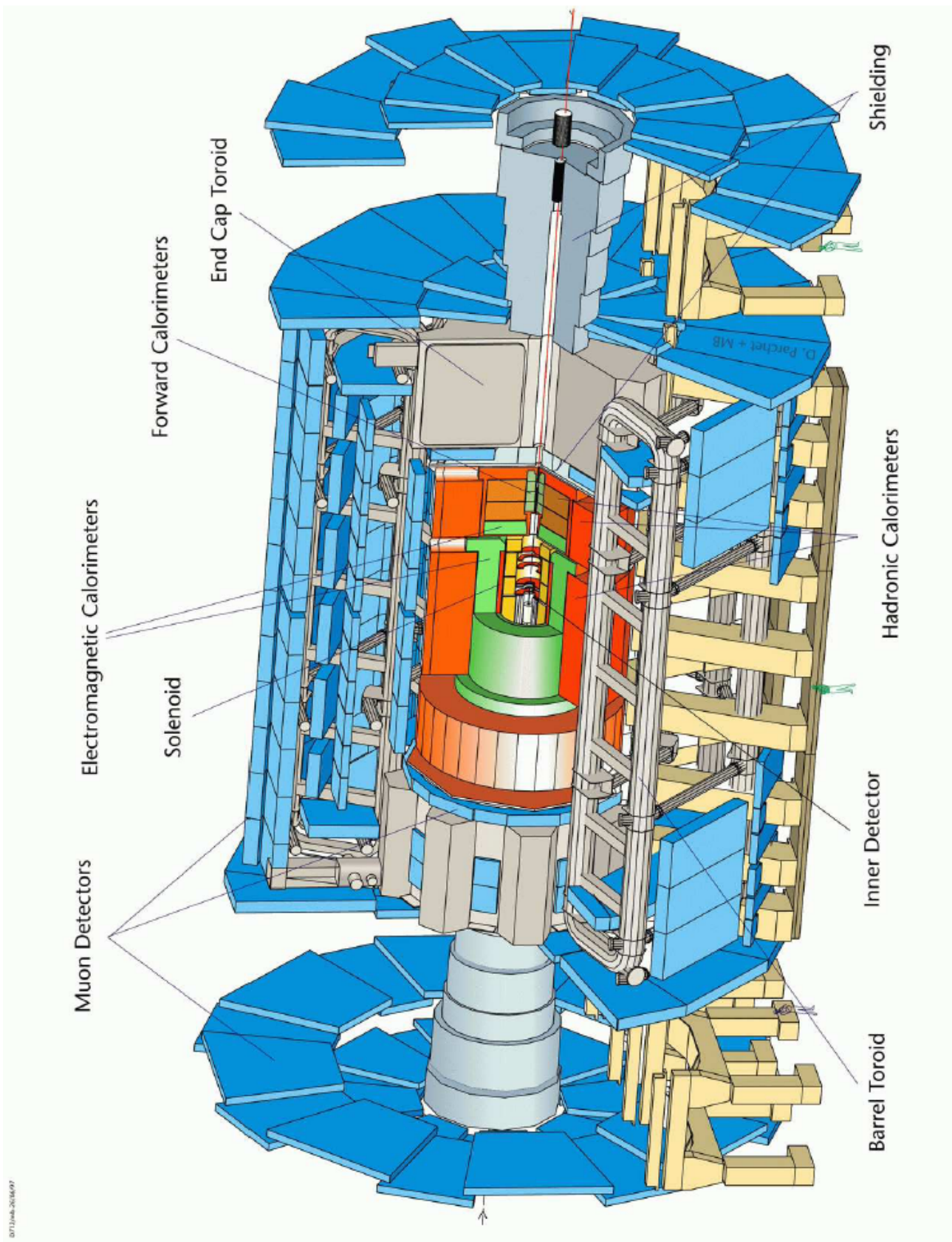


Figure 2: The ATLAS detector [8].

A superconducting solenoid generates the magnetic field in the inner region of the detector, while eight large air-core superconducting toroids are placed outside the calorimetric system, and provide the magnetic field for the external muon spectrometer[8].

The Magnet System

The overall dimensions of the ATLAS magnet system are 26 m in length and 22 m in diameter. In the end-cap region, the magnetic field is provided by the two toroid systems (ECT) inserted in the barrel toroid (BT) and lined up with the central solenoid (CS). The CS provides the inner trackers with a field of 2T (2.6T at the solenoid surface). Being the CS in front of the calorimetric system, its design was carefully tuned in order to minimize the material and not to produce any degradation of the calorimeter performance. As a consequence of this constraints, the CS and the barrel EM calorimeter share the same vacuum vessel. The operating current of the solenoid is 7.6 kA. The magnetic field generated by the BT and ECT have peak values of 3.9 and 4.1 T respectively. The eight coils of the BT, as well as the 16 coils of the ECT are electrically connected in series and powered by 21kA power supply. The magnets are cooled by a flow of helium at 4.5K. All the coils are made of a flat superconducting cable located in an aluminium stabilizer with rectangular shape [2,7,8].

The Inner Detector

The Inner Detector (Figure 3.) is entirely contained inside the Central Solenoid, which provides a magnetic field of 2 T. The high track density expected to characterize LHC events calls for a careful design of the inner tracker. In order to achieve the maximum granularity with the minimum of material, it has been chosen to use two different technologies: semiconductor trackers in the region around the vertex are followed by a straw tube tracker.

The semiconductor tracker (SCT) is divided in two subdetectors: a pixel detector and a silicon microstrip detector. The total number of precision layers is limited by the quantity of material they introduce and also because of their cost. The three pixel layers in the barrel have a resolution of 12 μm in $R\phi$ and 66 μm in Z . In the endcaps the five pixel disks on each side provide measurements in $R\phi$ and R with resolutions of 12 μm and 77 μm respectively. The innermost layer of pixel detectors in the barrel is placed at about 4 cm from the beam axis, in order to improve the secondary vertex measurement capabilities.

The SCT detector uses small angle (40 mrad) stereo strips to measure positions in both coordinates ($R\phi$ and Z for the barrel, R and $R\phi$ for the endcaps). For each detector layer one set of strips measures Z . The resolutions obtained in the barrel are 16 μm and 580 μm for $R\phi$ and Z respectively, while in the endcaps the resolutions are 16 μm in $R\phi$ and 580 μm in R .

The straw tubes are parallel to the beam in the barrel while in the endcaps they are placed along the

radial direction. Each straw tube has a resolution of $170\ \mu\text{m}$, and each track crosses about 36 tubes. In addition to this, the straw tube tracker can also detect the transition-radiation photons emitted by electrons crossing the xenon-based gas mixture of the tubes, thus improving the ATLAS particle identification capabilities.

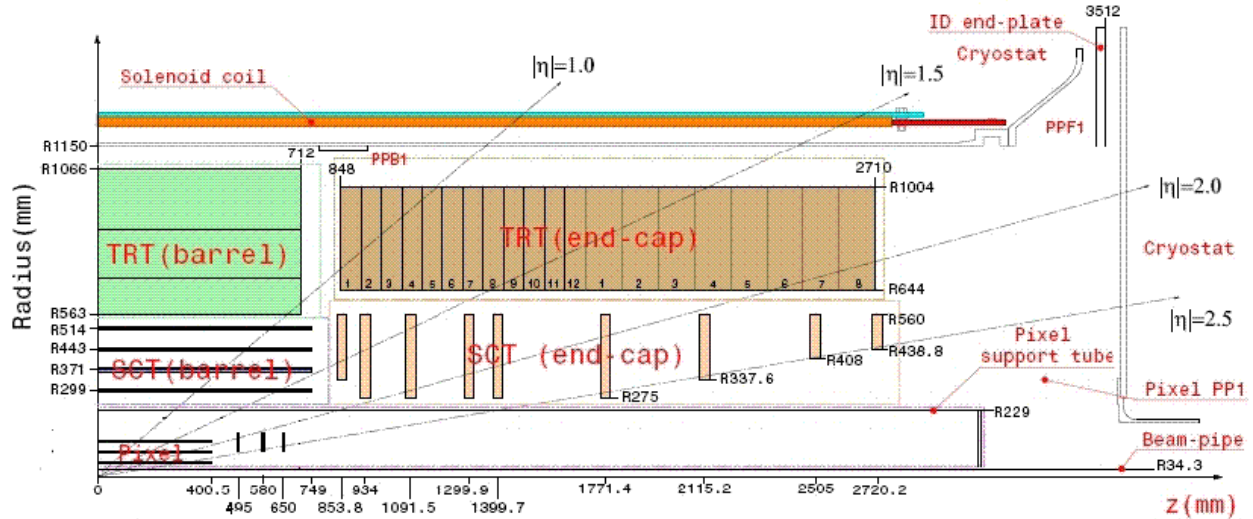


Figure 3: ATLAS Inner Detector (ID) [8].

The EM Calorimeter

The EM calorimeter is divided in three parts: barrel ($\eta < 1.7$) and two endcaps ($1.375 < \eta < 3.2$). The barrel calorimeter is divided in two half barrels, with a small (6mm) gap between them at $z = 0$. The endcap calorimeters are made up of two coaxial wheels each. The layout of the EM calorimeter, together with the hadronic one. The EM calorimeter is a Liquid Argon detector with lead absorber plates and Kapton electrodes. In order to provide a full coverage in, an accordion geometry was chosen for the internal layout of the calorimeter. The lead absorber layers have variable thickness as a function of and has been optimized to obtain the best energy resolution. The LAr gap on the contrary has a constant thickness of 2.1 mm in the barrel. The total thickness is $> 24 X_0$ in the barrel and $> 26 X_0$ in the endcaps.

In the region with $\eta < 2.5$ the EM calorimeter is longitudinally divided in three sections. The first region, is meant to work as a preshower detector, providing particle identification capabilities and precise measurement in η . It has a thickness of $6 X_0$ constant as a function of η , is read out with strips of 4mm in the η direction [8].

The Hadronic Calorimeter

The region with $\eta < 4,9$ is covered by the hadronic calorimeters using different techniques, taking into account the varying requirements and radiation environment over this large range. The range $\eta < 1,7$, corresponding to the barrel calorimeter, is equipped with a calorimeter (TC) based on the iron/scintillating tile technology. Over the range $1,5 < \eta < 4,9$, Liquid Argon calorimeters were chosen. In this region the hadronic calorimetry is segmented into an Hadronic End-Cap Calorimeter (HEC), extending up to $\eta < 3,2$ and a High Density Forward Calorimeter (FCAL) covering the region with highest η . Both the HEC and the FCAL are integrated in the same cryostat housing the EM end-caps calorimetry.

The thickness of the calorimeter has been carefully tuned in order to provide good containment of hadronic showers and reduce to the minimum the punch through into the muon system. At $\eta = 0$ the total thickness is 11 hadronic interaction lengths, including the contribution from the outer support. This has been shown by measurements and simulation to be sufficient to reduce the punch through to just prompt or decay muons, while 10 of active calorimeter provide good resolution for high energy jets. This characteristics, together with the large coverage, will guarantee an accurate E_{miss} measurement, which is an important parameter in the signatures of many physics processes[8].

Trigger

The ATLAS trigger has three levels of event selection: Level 1 (LVL1) which is hardware-based using ASICs and FPGAs, the Level 2 (LVL2) and Event Filter (EF) (collectively referred to as the High Level Trigger or HLT) based on software algorithms analysing the data on large computing farms. The three levels of the ATLAS trigger system must reduce the output event storage rate to 200 Hz (about 300 MB/s) from an initial LHC bunch crossing rate of 40 MHz. It is evident from

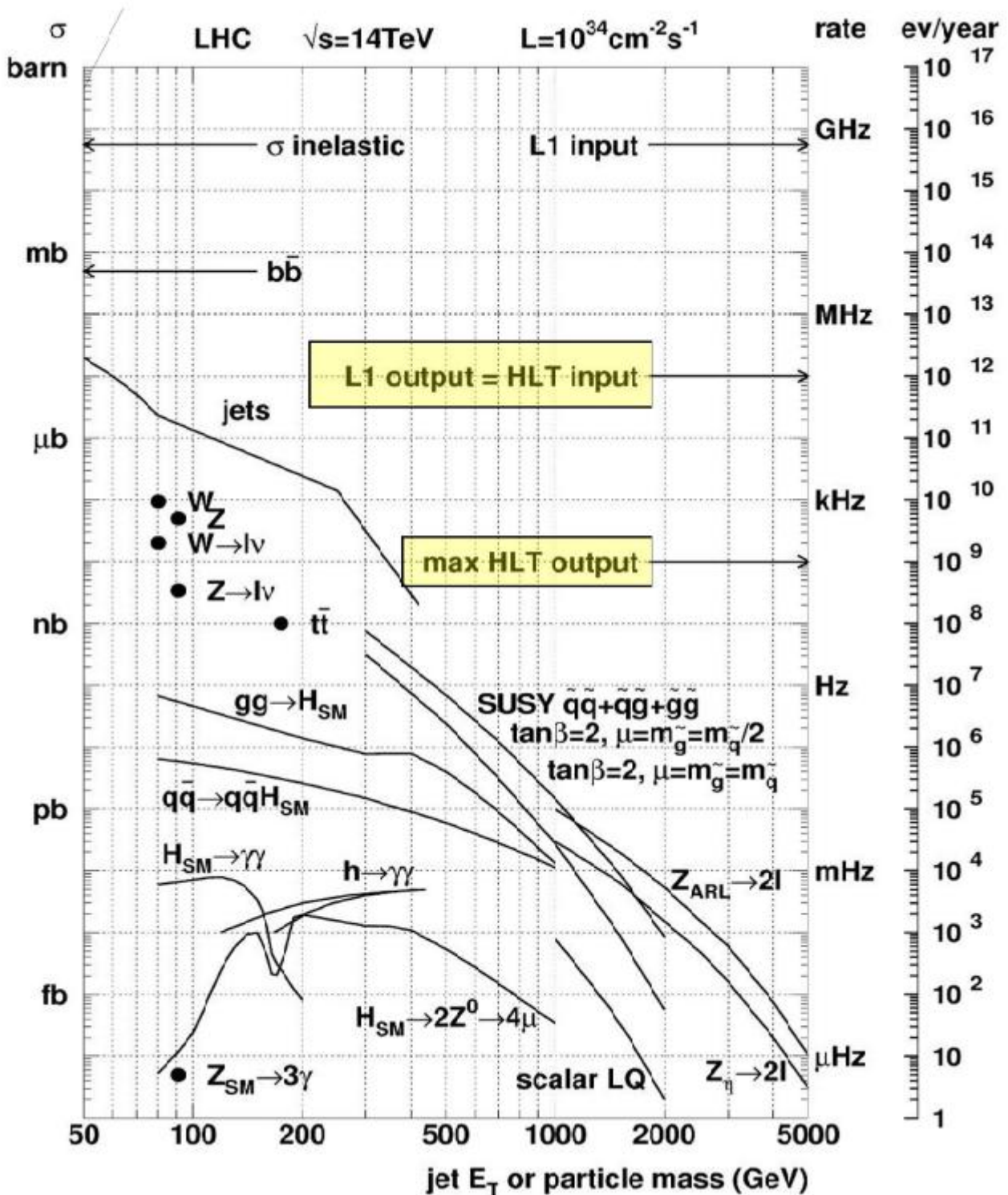


Figure 4: Expected event rates for several physics processes at the LHC design luminosity.

Figure 4. that large rejection against QCD processes is needed while maintaining high efficiency for low cross section physics processes that include searches for new physics. During the ATLAS startup phase, where low luminosity conditions ($10^{31} \text{ cm}^{-2} \text{ s}^{-1}$) are expected to prevail, the focus of the trigger selection strategy will be to commission the trigger and the detector and to ensure that established Standard Model processes are observed. It is therefore important to deploy loose selection criteria at each stage. In early operations many triggers will operate in pass-through mode, which entails executing the trigger algorithms but accepting the event independent of the algorithmic decision. This allows the trigger selections and algorithms to be validated to ensure that they are robust against the varying beam and detector conditions that are hard to predict before data-taking. As the luminosity increases, the use of higher thresholds, isolation criteria and tighter selections at HLT become necessary to reduce the background rates while achieving selection of interesting physics with high efficiency[1,2,8].

Level 1 trigger

The Level 1 trigger system receives data at the full LHC bunch crossing rate of 40 MHz and must make its decision within $2.5 \mu\text{s}$ to reduce the output rate to 75 kHz (40 kHz during ATLAS start-up). The L1 trigger has dedicated access to data from the calorimeter and muon detectors. The LVL1 calorimeter trigger decision is based on the multiplicities and energy thresholds of the following objects observed in the ATLAS Liquid Argon and Tile calorimeter sub-system: Electromagnetic (EM) clusters, taus, jets, missing transverse energy E_{miss} , scalar sum E_T in calorimeter, and total transverse energy of observed LVL1 jets. These objects are computed by the LVL1 algorithms using the measured E_T values in trigger towers of 0.1×0.1 granularity in $\Delta\eta \times \Delta\phi$. The LVL1 muon trigger uses measurement of trajectories in the different stations of the muon trigger detectors: the Resistive Plate Chambers (RPC) in the barrel region and the Thin Gap Chambers (TGC) in the endcap region. The input to the trigger decision is the multiplicity for various muon p_T thresholds. There are a limited number of configuration choices that are available at LVL1. The most common difference between configuration choices is the amount of transverse energy or momentum required, so we refer to these configurations as “thresholds,” but note that in addition to the E_T threshold condition, three different isolation criteria can be applied for LVL1 EM and tau objects, and three different window sizes can be specified for LVL1 jet objects. Table 1 gives the number of these so-called thresholds that can be set for each object type. The total number of thresholds allowed for EM and tau objects is 16, where 8 are dedicated to be EM objects and 8 can be configured to be either EM or tau objects. The forward jets have four thresholds that can be set independently in each of the detector arms.

Object	EM	Taus	Jets	For. Jets	\cancel{E}_T	$\sum E_T$	$\sum E_T(jets)$	$\mu_{\leq 10} \text{ GeV}$	$\mu_{> 10} \text{ GeV}$
# of thresholds	8 - 16	0 - 8	8	4+4	8	4	4	3	3

Table 1: Number of L1 thresholds that can be set for each LVL1 object type at any given time[1]

The total number of allowed LVL1 configurations (also called LVL1 items) that can be deployed at any time is 256. Each of these LVL1 items, programmed in the Central Trigger Processor (CTP), is a logical combination of the specified multiplicities of one or more of the configured LVL1 thresholds. As an example L1_EM25i and L1_EM25 (A single LVL1 EM object with $E_T > 25 \text{ GeV}$ with and without isolation respectively) uses two LVL1 EM thresholds while L1_2EM25i (Two L1 isolated EM object with $E_T > 25 \text{ GeV}$) uses the same LVL1 threshold as the L1_EM25i item. Furthermore, for each of the 256 LVL1 items, a prescale factor N can be specified (where only 1 in N events is selected and passed to the HLT for further consideration). As the peak luminosity drops during a fill, the LVL1 prescale value can be adjusted to keep the output bandwidth saturated without stopping and restarting a data-taking run, if desired [1,3,6,8].

Level 2 trigger

The L2 trigger is software-based, with the selection algorithms running on a farm of commodity PCs. The selection is largely based on regions-of-interest (RoI) identified at LVL1 and uses fine-grained data from the detector for a local analysis of the LVL1 candidate. A seed is constructed for each trigger accepted by LVL1 that consists of a p_T threshold and an η - ϕ position. The LVL2 algorithms use this seed to construct an RoI window around the seed position. The size of the RoI window is determined by the LVL2 algorithms depending on the type of triggered object (for example, a smaller RoI is used for electron triggers than for jet triggers). The LVL2 algorithms then use the RoI to selectively access, unpack and analyse the associated detector data for that η - ϕ position. The ability to move, unpack, and analyse the local data only around the seed position greatly reduces both the processing times and the required data bandwidth. The LVL2 algorithms provide a refined analysis of the LVL1 features based on fine-grained detector data and more optimal calibrations to provide results with improved resolution. They provide the ability to use detector information that is not available at LVL1, most notably reconstructed tracks from the Inner Detector. The information from individual sub-systems can then be matched to provide additional rejection and higher purity at LVL2. For each LVL1 RoI, a sequence of LVL2 algorithms is executed which compute event feature quantities associated with the RoI. Subsequently, a coherent set of selection criteria is applied on the derived features to determine if the candidate object should

be retained. The LVL2 farm will consist of around 500 quad-core CPUs. On average, the LVL2 can initiate the processing of a new event every 10 μ s. The average processing time available for LVL2 algorithms is 40 ms, which includes the time for data transfers. The LVL2 system must provide an additional rejection compared to LVL1 of about 40 to reduce the output rate down from 75 (40) kHz to 2 (1) kHz during nominal (startup) operations [1,3,6,8].

Event Filter

The final on-line selection is performed by software algorithms running on the Event Filter (EF), a farm of processors that will consist 1800 dual quad-core CPUs. The EF receives events accepted by LVL2 at a rate of 2 kHz (1 kHz) during nominal (startup) operations and must provide the additional rejection to reduce the output rate to 200 Hz, corresponding to about 300 MB/s. An average processing time of 4 μ s per event is available to achieve this rejection. The output rate from the Event Filter is limited by the offline computing budget and storage capacity.

As in LVL2, the EF works in a seeded mode, although it has direct access to the complete data for a given event as the EF selection is performed after the event building step. Each LVL2 trigger that has been accepted can be used to seed a sequence of EF algorithms that provide a more refined and complete analysis. Unlike LVL2, which uses specialized algorithms optimized for timing performance, the EF typically uses the same algorithms as the offline reconstruction. The use of the more complex pattern recognition algorithms and calibration developed for offline helps in providing the additional rejection needed at the EF [1,3,6,8].

Trigger rate

Trigger rates have been estimated using a sample of simulated events. The design of a specific trigger menu often requires several iterations of selection optimization to ensure that the output rate is within allowed bandwidths and that interesting physics is triggered with high efficiency.

The first step in approximating trigger rates is to choose an appropriate input simulation sample. Most trigger selections are dominated by backgrounds from common processes, so samples with large physics cross-sections are generally used. However, these typically contain very few events that satisfy the trigger criteria and hence a very large number of events are required to obtain adequate statistical uncertainties on the estimated rates. In order to design the trigger menu for a luminosity of $10^{31} \text{ cm}^{-2} \text{ s}^{-1}$, a minimum bias dataset containing seven million non-diffractive events with a cross-section of approximately 70 mb was used. To estimate the trigger rates with comparable statistical uncertainties for higher luminosities would require prohibitively large

generated samples, hence other approaches are being pursued. These include using a combination of QCD and minimum bias event samples or alternatively using the so-called enhanced bias sample. The enhanced bias sample is a loosely filtered minimum bias sample requiring the lowest L1 pT thresholds for muon, EM, or jet to have been fulfilled. Only events that pass the filtering process are reconstructed, resulting in a much more effective use of the computing resources. In addition to QCD processes, other high cross-section physics processes, such as W and Z boson production, need to be considered for estimating trigger rates at very high luminosities. Although such simulated samples provide a reasonable starting point to establish a data taking menu, these trigger menus will evolve as our understanding of the detector and trigger evolve, and as the physics requirements mature. Once data taking operations begin, dedicated data samples for further menu optimization and rate estimations will be collected.

In order to compute the initial trigger rates, the full trigger simulation (LVL1, LVL2, and EF) is executed on a minimum bias data sample generated with PYTHIA and simulated with realistic detector effects in Geant4 [1,3,6,8].

Data streams

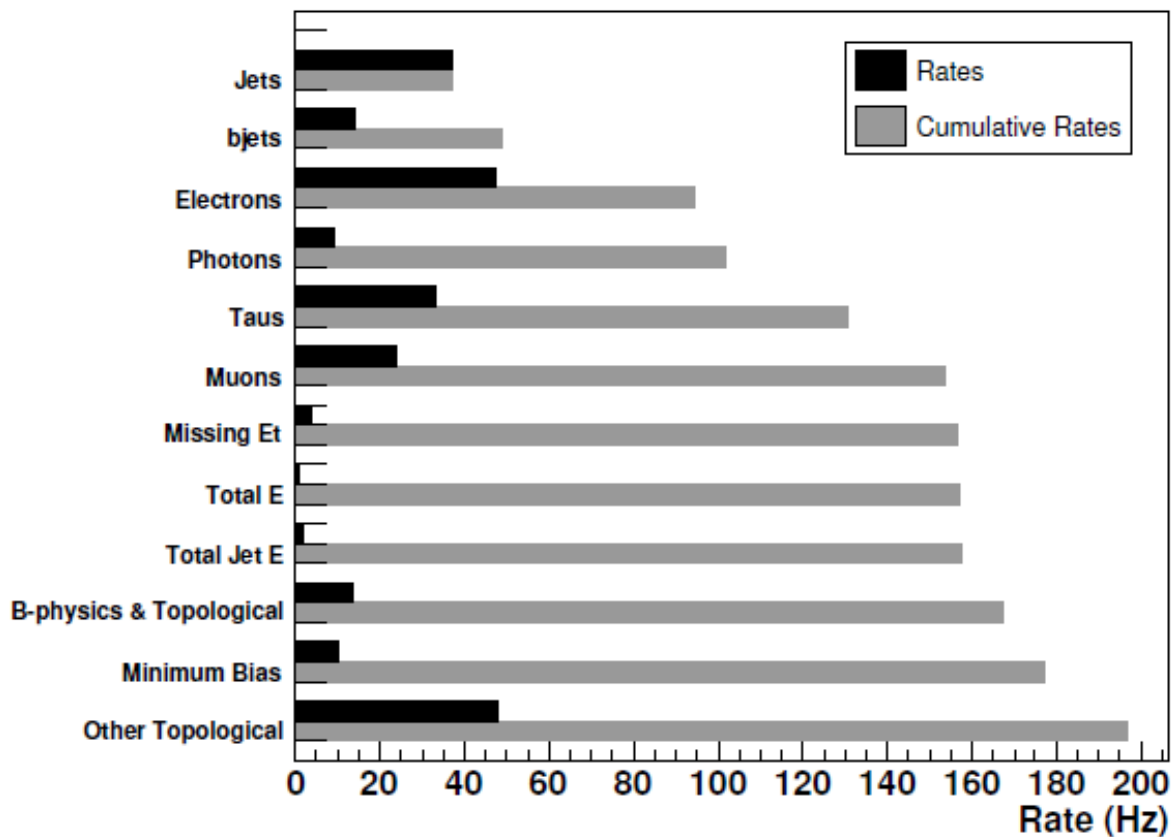


Figure 5: HLT unique (black) and cumulative (gray) estimated rates at $10^{31} \text{ cm}^{-2} \text{ s}^{-1}$ for different trigger

ATLAS has adopted an inclusive streaming model whereby raw data events can be streamed to one

or more files based on the trigger decision. A proposed initial streaming configuration consists of four raw data streams called egamma, jetTauEtmis, muons, and minbias. Each stream consists of events that pass one or more trigger signatures. The stream names indicate the type of trigger signatures they will contain [1].

Data production and preparation

Data production by Monte Carlo

Analysis presented in this work was done using Pythia 8, which is one of leading MC generators used in HEP. Generation of events was performed on the grid. The JobOption file was made and Z boson production with it's two-muon decay was allowed. Settings of Pythia are shown in the text below. Number of events was set to 10 000 to gather sufficient statistics and for further analysis. Athena release 15.3.0 was used for production.

```
topAlg.Pythia.PythiaCommand = [ "pyinit win 7000.", # 7 TeV, CMS energy
```

In this line CMS energy of 7 TeV was declared, it is expected energy of beam collisions in early LHC physics programme.

```
    "pysubs msel 0",           # Users decay choice.
    "pydat1 parj 90 20000",    # Turn off FSR.
    "pydat3 mdcy 15 1 0",     # Turn off tau decays.
    "pypars mstp 81 20",      # turn off multiple interactions
```

These lines simplify analysis by removing multiple interactions from event collisions.

Z production:

```
    "pysubs msub 1 1",        # Create Z bosons.
    "pysubs ckin 1 60.0",     # Lower invariant mass.
    "pydat3 mdme 174 1 0",
    "pydat3 mdme 175 1 0",
    "pydat3 mdme 176 1 0",
    "pydat3 mdme 177 1 0",
    "pydat3 mdme 178 1 0",
    "pydat3 mdme 179 1 0",
    "pydat3 mdme 182 1 0",    # Switch for Z->ee.
```

```
"pydat3 mdme 183 1 0",  
"pydat3 mdme 184 1 1", # Switch for Z->mumu.  
"pydat3 mdme 185 1 0",  
"pydat3 mdme 186 1 0", # Switch for Z->tautau.  
"pydat3 mdme 187 1 0"]
```

For the calculation of efficiencies the data with the Z boson decaying into two muons in every event are required.

In end of this production the dataset user09.PetrGallus.123456.Zmumu7TeV.evgen.pool.v1 was produced which contained collection of produced particles.

Data conversion

It was necessary to perform a GEANT4 simulation and digitization of particle collision to simulate the effects of the detector, resultant RDO (Raw Data Object) file was produced. For this task job transformation in pAthena was used and ran on the grid. Standard csc_simul_trf.py transformation was used.

```
pathena --split=100 --nFilesPerJob=1 --trf "csc_simul_trf.py %IN %OUT.hits.pool.root  
%OUT.rdo.pool.root 100 0 1324354656 ATLAS-GEO-08-00-00 100 1000"  
--inDS user09.PetrGallus.123456.Zmumu7TeV.evgen.pool.v1  
--outDS user09.PetrGallus.123456.Zmumu7TeV.RDO.v1
```

In this command standard geometry of Atlas ATLAS-GEO-08-00-00 was used, input and output datasets were declared. Simulation and reconstruction was run on parallel, 100 jobs had each 100 events which makes 10000 events in total.

Making ntuples and AOD

For the reconstruction part, the job transformation on the grid takes considerable amount of time and it has many technical difficulties. So it was done on a local machine. For reconstruction and NTUPLE production t these 3 packages were used:

InDetRecExample (InDetRecExample-01-17-44)

TrkGlobalChi2Fitter (TrkGlobalChi2Fitter-00-03-19)

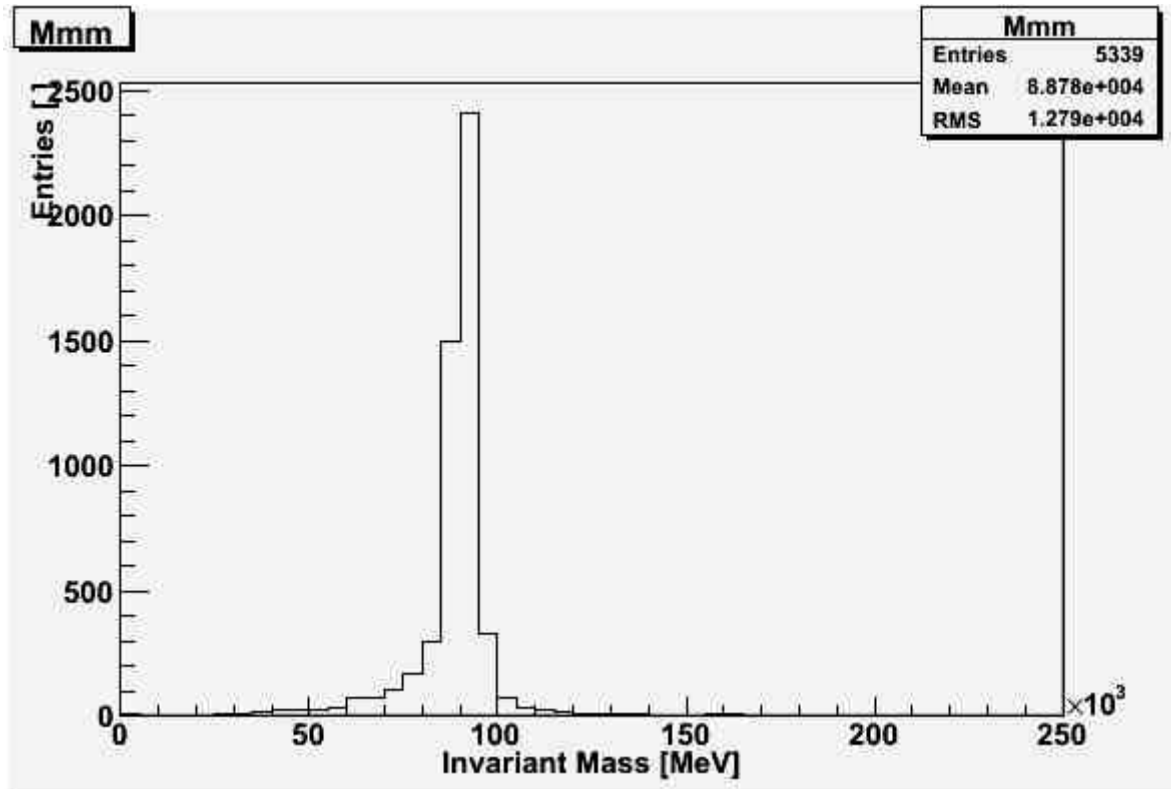
TrkValTools (TrkValTools-00-07-19)

For transformation of RDO files to the NTUPLEs the most important package was InDetRecExample, jobOption.py were default from it's share directory. This file was modified to make output NTUPLEs as well as AOD files, every output file has 250 events after merging. This NTUPLE files can be read and processed by pure ROOT.

Data analysis

Data processing of AOD files

In this part of analysis the AnalysisExamples (AnalysisExamples-00-20-45) package was used for converting AOD file to the root file. I did some modification of the package and used it to process data produced locally and also to process an official validated data set valid1.105145.PythiaZmumu.recon.AOD.e380_s559_r730. The official dataset used ATLAS-GEO-08-00-01 geometry and it was produced by same job transformation as was used in the case of local generation. In the comparison of locally produced data and the validated dataset there are were not any easily-visible contradictions. So for further analysis locally produced data were used. Histogram of invariant mass of two muons from decay of Z boson follows. It was produced by ZmumuZeeOnESD package.



Histogram 1: Invariant mass of two muons with highest p_t .

In Histogram 1. we can see that after all full chain of production of data we still have a sharp peak of Z boson and it can be fit well by Breit-Wigner distribution. Mass peak is where it is expected.

Data processing of ntuples files

For analysis of the trigger I used the root macro, which was written by my colleague Michal Marcisovsky and I did some modifications to it to suit my needs. This macro does plot histograms of η , p or p_t in dependence of LVL1 trigger used in the event.

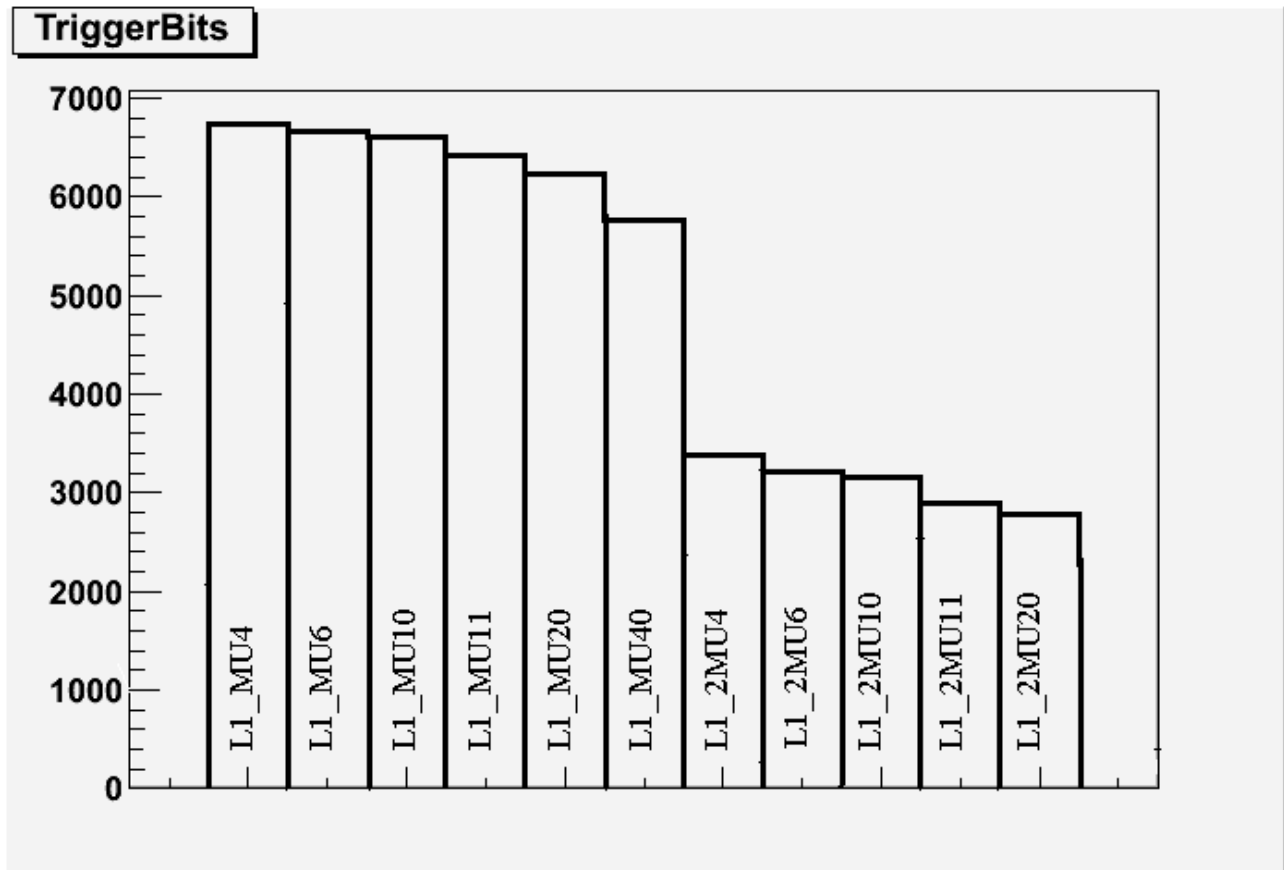
Because the Z to $\mu\mu^+$ decay was chosen, study of muon triggers was put in focus. There are several trigger menus, early physics menu for luminosity of 10^{31} was chosen.

Muon LVL1 available in the early physics trigger menu are:

L1_MU4	L1_MU6	L1_MU10	L1_MU11
L1_MU20	L1_MU40	L1_2MU4	L1_2MU6
L1_2MU10	L1_2MU11	L1_2MU20	L1_2MU4_MU6

Number in the end of trigger identifier is energy threshold in GeV. For example L1_MU6 trigger will mark every event with a muon with a momentum higher than 6 GeV. Furthermore, number in front of muon declaration in the name of trigger such as “2MU” implies number of muons with this

threshold.



Histogram 2: Number of triggered events for muon triggers, total number of events is 7500.

The numbers (bits) of triggered events of LVL1 muon triggers are displayed in Histogram 2. It is clearly visible that increasing the thresholds lowers the number of events that have passed. The trigger efficiencies are calculated by dividing the histograms of events with this trigger by histograms with all events.

Event distribution

Before efficiencies of triggers are calculated, we will have a look at the observable quantities. First of them is momentum p (Figure 3.) We can see that most of muons have momentum between 20 GeV and 80 GeV. That is why we have big error bars in efficiencies for p outside of this area. Another observable is pseudorapidity η of the track (Figure 4), it is symmetric and the most of muons have $|\eta| < 2.5$. That is because of detector geometry.

Theta (θ) has symmetric distribution with small peak in center and two in sides (Figure 5). That we can interpret like continuation of beam.

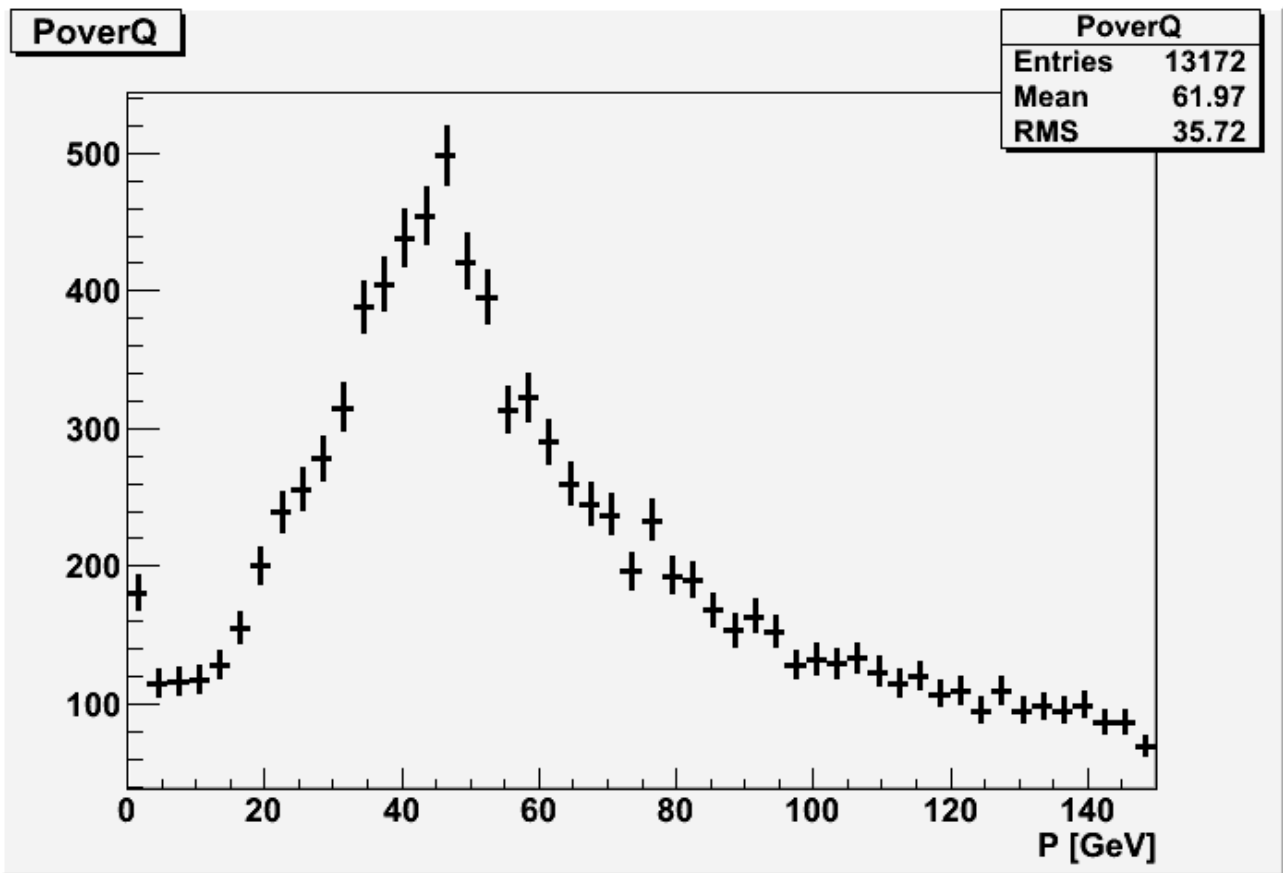


Figure 6: Distribution of muons as function of p .

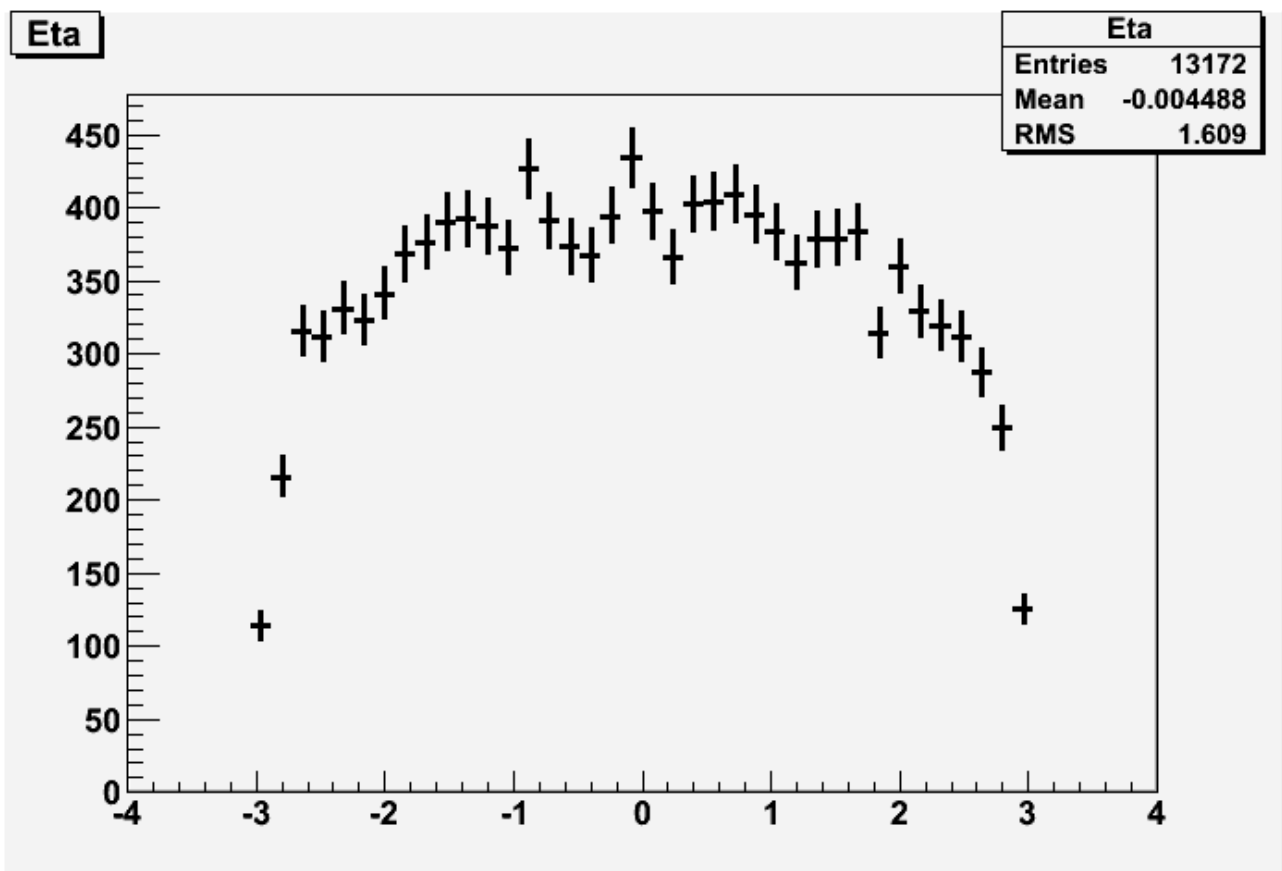


Figure 7: Distribution of muons as function of η .

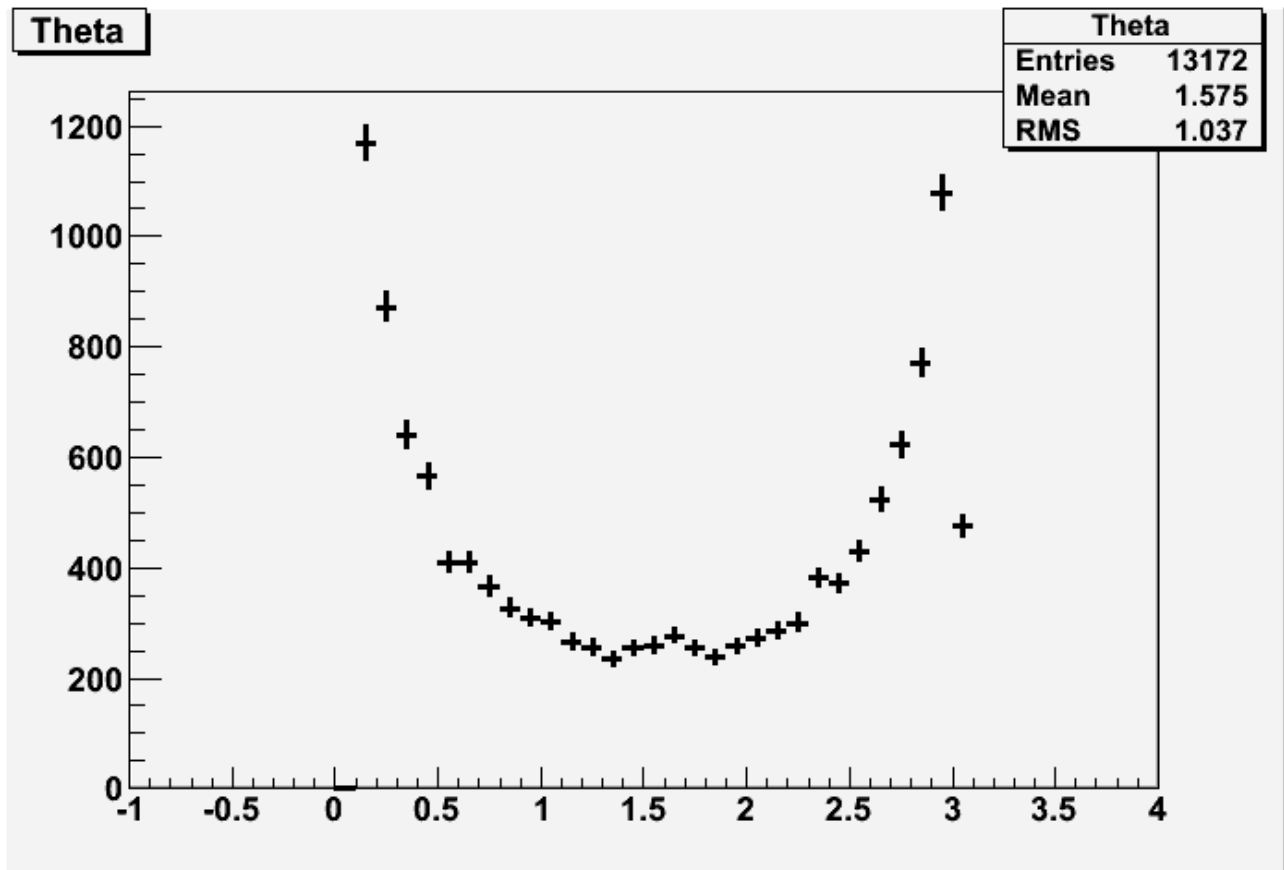


Figure 8: Distribution of muons as function of θ .

L1_MU20 item

This trigger demands that muon has momentum higher than 20 GeV. Muons with this energy are derivable from decays of particles with high invariant mass such as Z boson or W boson or require a large Lorentz boost [4,5]. In Figure 9. we can see that efficiency is very close to one for muons with momentum higher than 20 GeV. Data in energy 1 to 5 GeV are made by sorting collections in script, it was hard to resolve which muon in event was triggered so every one of them was counted in. Next histogram (Figure 10.) shows how trigger efficiency depends on the pseudorapidity. We can see that it is symmetric and it has few pits around $\eta=1$ and 0. It is caused by the detector geometry and around $\eta = 0$ it is probably caused by the trigger itself. When we have a look at the Figure 3. (the Inner Detector) it is visible that at $\eta=1$ TRT Barrel ends and TRT Endcap starts and this is probable reason for the drop. Also measurement of particles with pseudorapidity higher than 2.5 is caused by ending of inner detector at this coordinate. Similar picture we can see in histogram of efficiency as a function of θ (Figure 11.). Next important distribution is function of p_T (Figure 12.), in which we see that it has same trend as function of momentum. It has slightly lower slope because of the relation between p_T and momentum. The important thing seen in this histogram is high efficiency for high p_T .

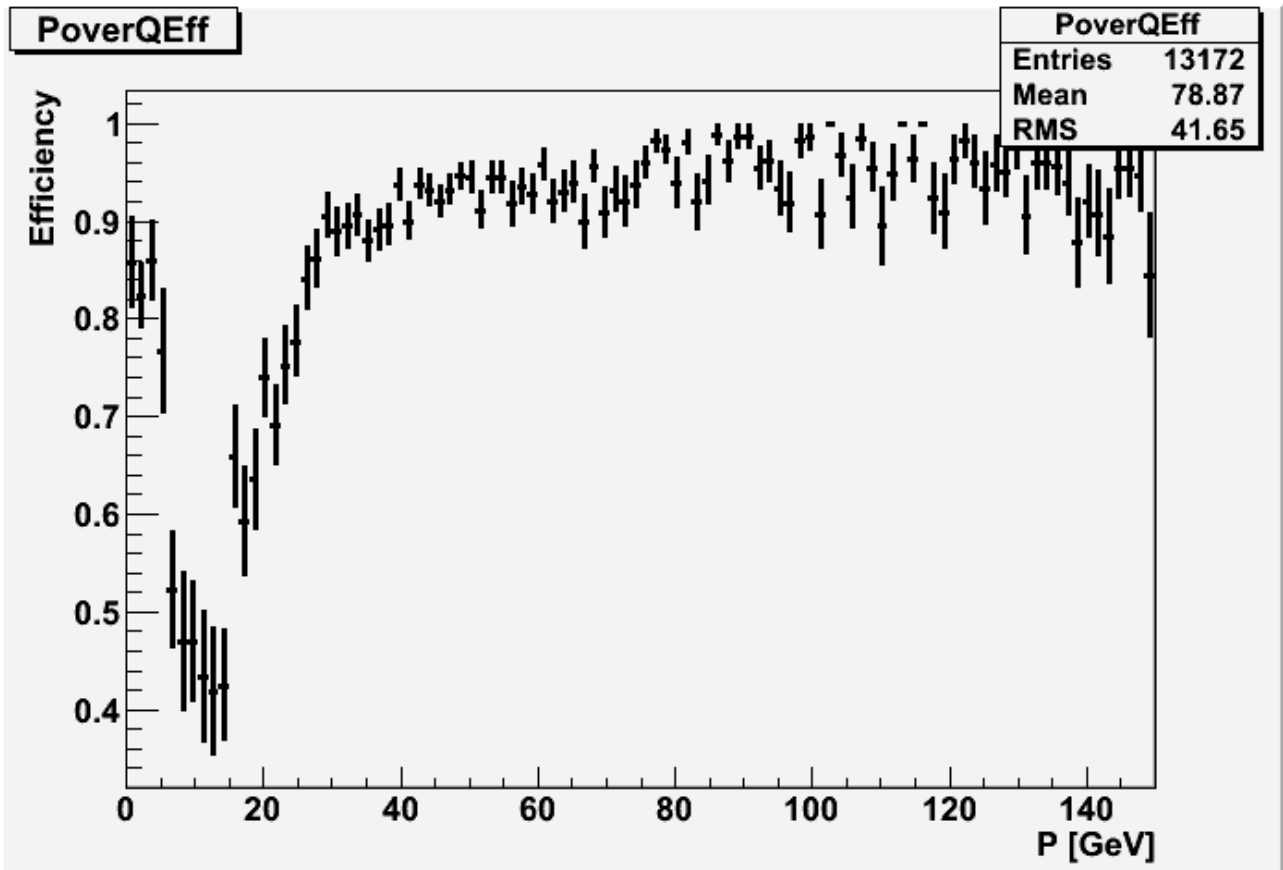


Figure 9: The efficiency of L1_MU20 as function of p .

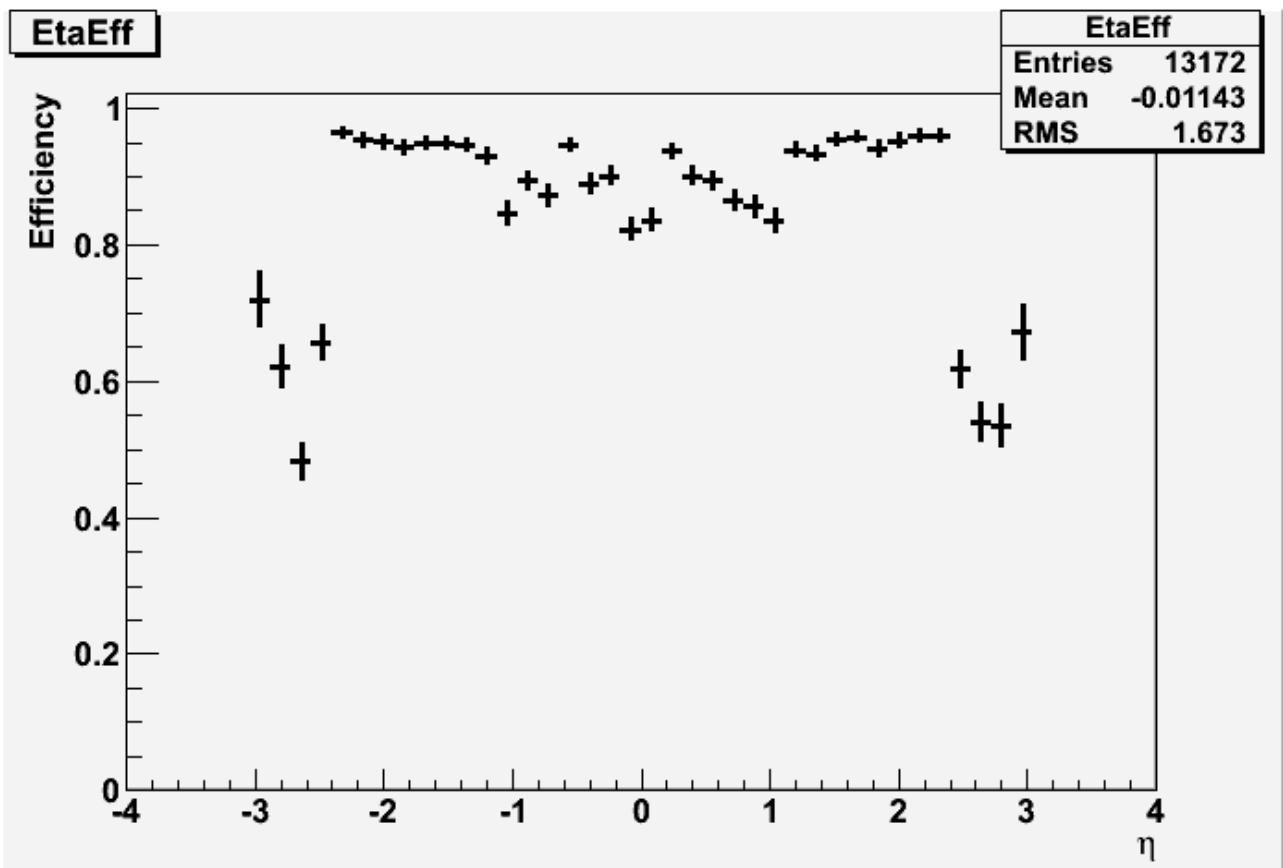


Figure 10: The efficiency of L1_MU20 as function of η .

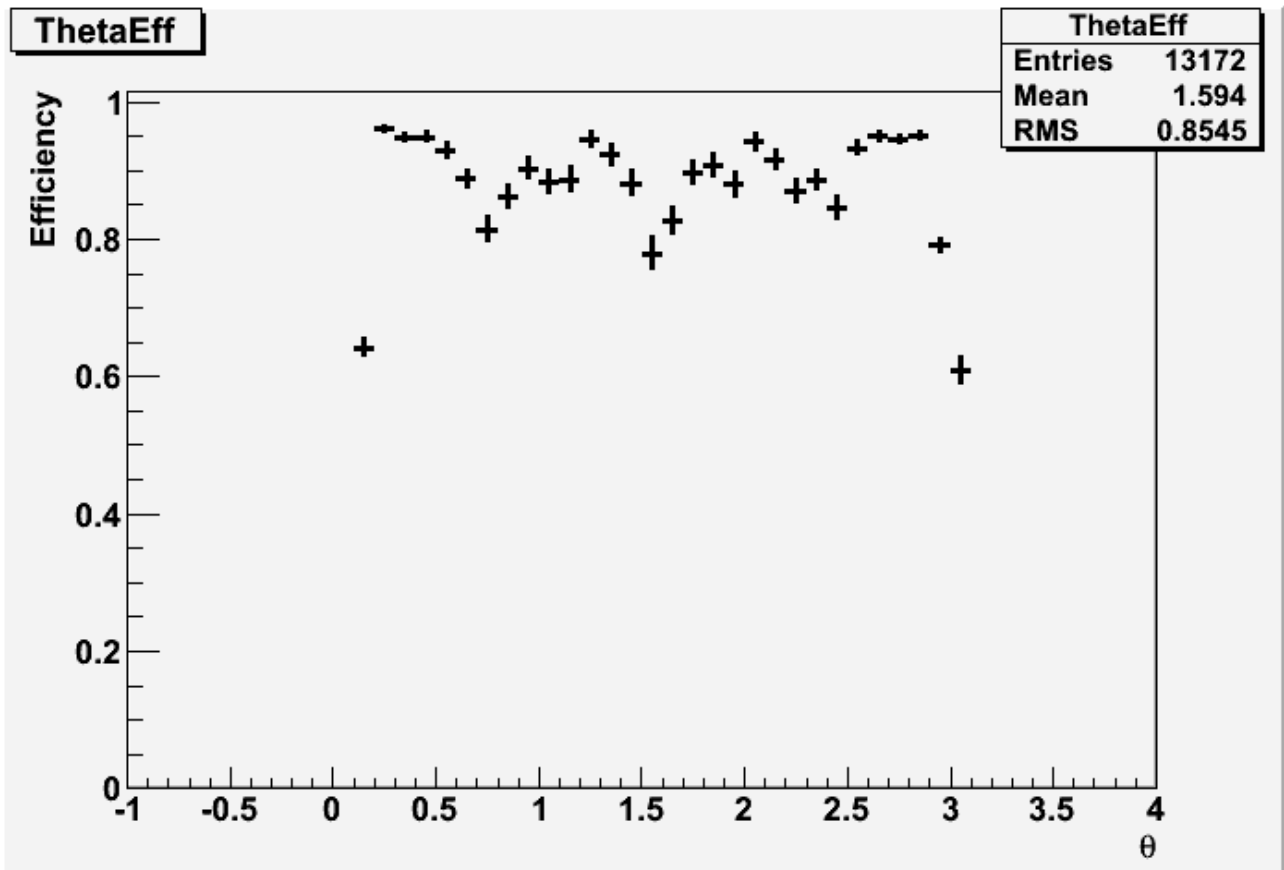


Figure 11: The efficiency of L1_MU20 as function of θ .

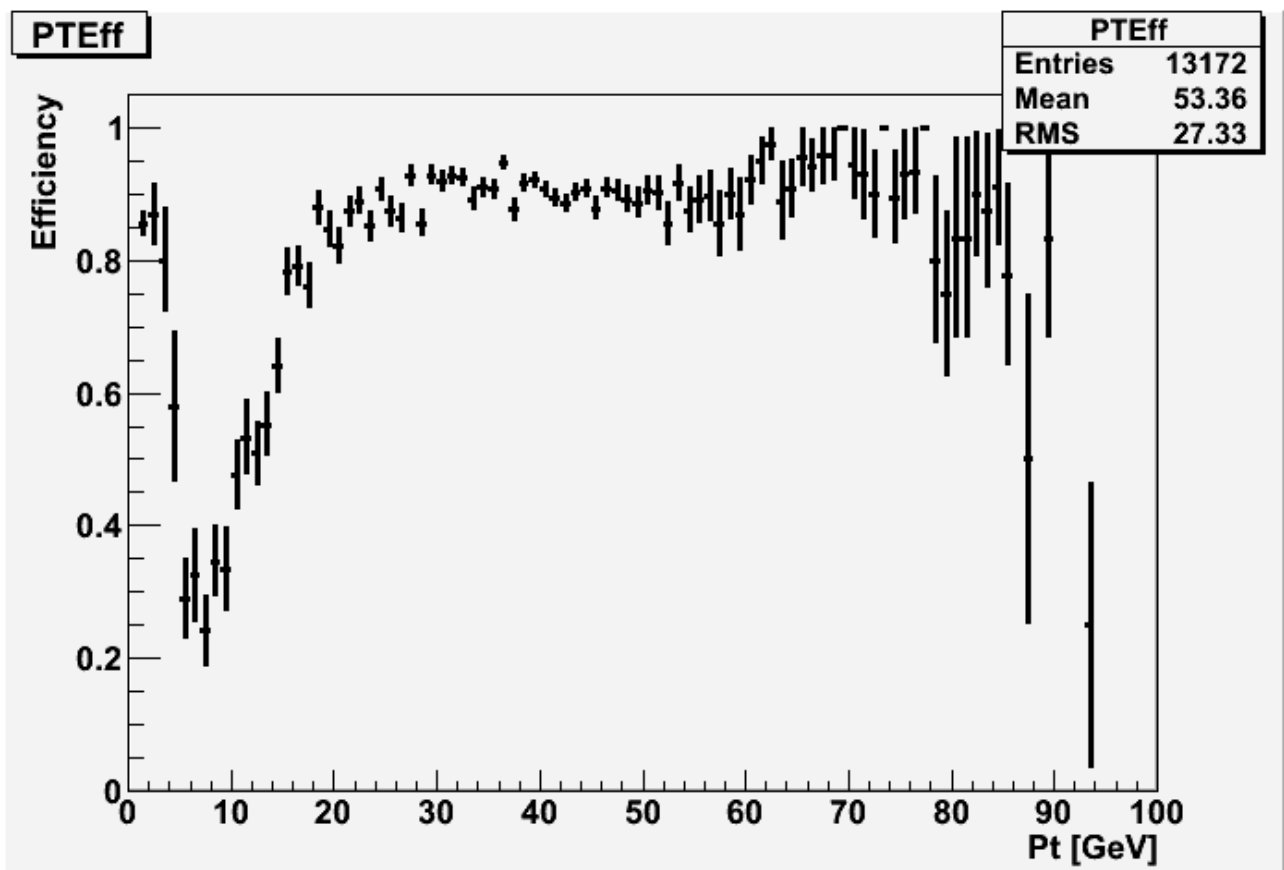


Figure 13: The efficiency of L1_MU20 as function of p_T .

L1_2MU20 item

I study this trigger to compare efficiencies of triggers and doing comparison in between one muon and two muons triggers. This trigger has the 20 GeV threshold in energy for two muons. As a first thing to say about this efficiencies is that they are much smaller than for L1_MU20, that is because two muons are needed. There is higher probability not to trigger both muons because of distribution of energy, detector angular cuts or misidentification. In L1_MU20 example we see that efficiencies are around 0.9, for double muon trigger efficiency dropped to about 0.6. In histogram for single muon trigger (Figure 13) we can see the dependence on momentum. First what we see is small efficiency around 20 GeV, that is because of cut of this trigger. We can compare it with same histogram for trigger L1_MU20, which we study earlier (Figure 9) and only difference is value of efficiency. Next histograms will show similar behavior for η and θ (Figure 14 and 15). In Figure 10. for single-muon case small drops in trigger effectivity are visible at around $\eta = 0$ and 1, in the case of two-muon trigger these drops are amplified due to the fact that trigger requires two muons. When there is one of those two muons in this pseudorapidity area, chances of not triggering it is much higher.

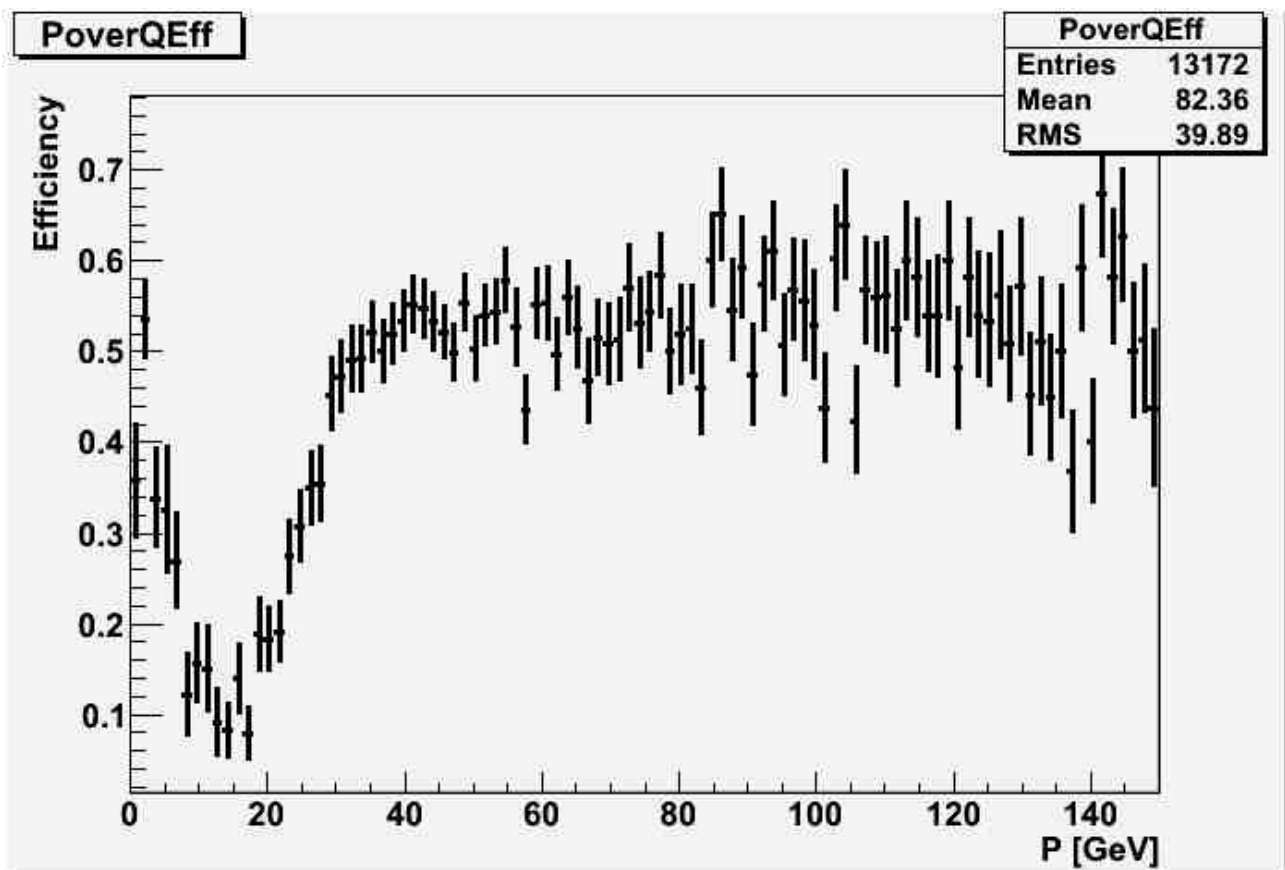


Figure 14: The efficiency of L1_2MU20 on dependency to momentum.

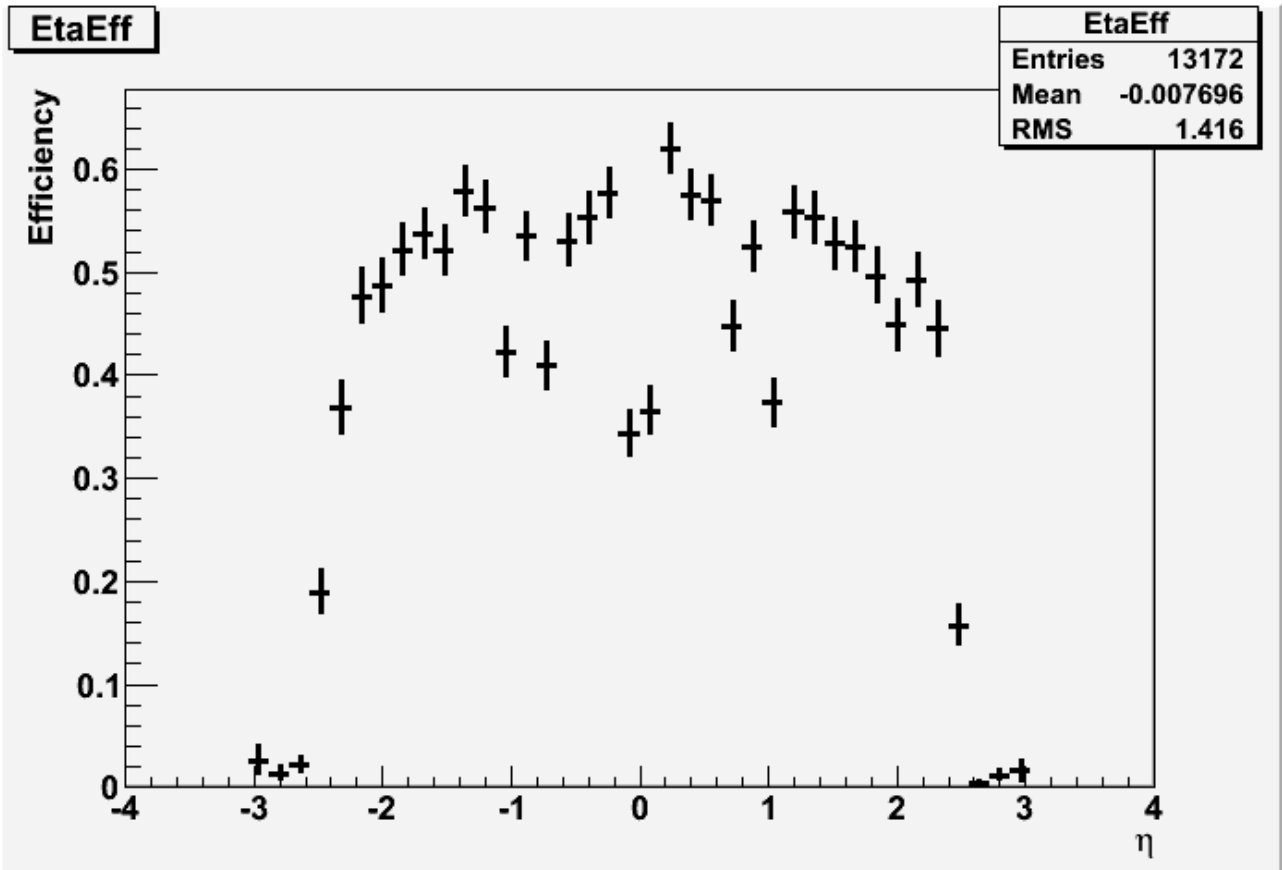


Figure 15: The efficiency of L1_2MU20 of dependency to η .

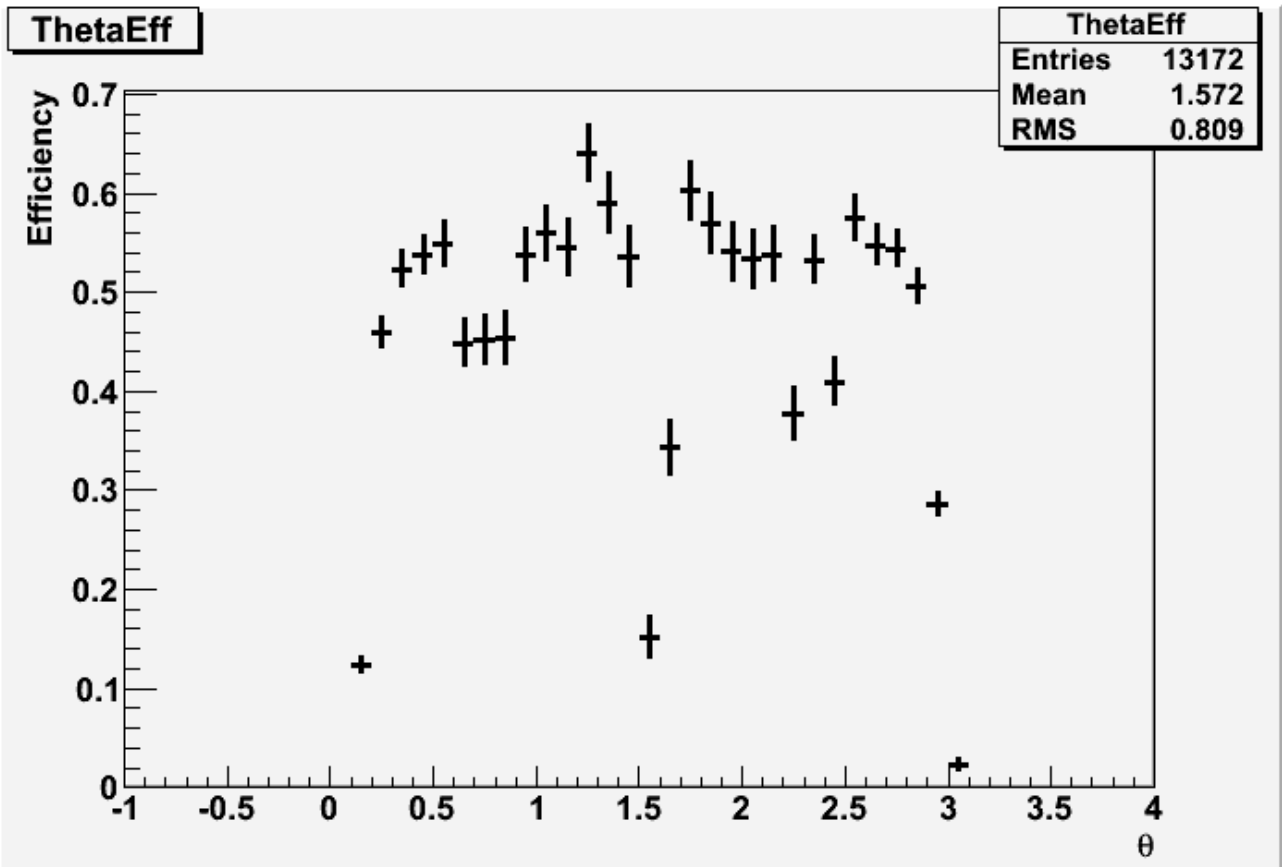


Figure 16: The efficiency of L1_2MU20 of dependency to θ .

Conclusions

In this work the efficiencies of the LVL1 muon trigger were discussed with reference decay of Z boson into two muons. Two triggers were examined, namely LI_MU20 and LI_2MU20. Muons in the selection must have momentum higher than 20 GeV. Single muon trigger has higher efficiency than double-muon trigger because of amplification of detector selection effects and angular cuts. Conclusions for this triggers are that the trigger works as expected.

For the trigger dependencies we found that for dependency to momentum it works as expected but for dependency to the pseudorapidity η and theta θ effectivity depend to the detector geometry. There are significant drops in $|\eta| = 1$ and also in $\theta \sim 1.7$ and 2.3 , this drops are probably caused by the detector geometry. The drops in $\eta = 0$ or $\theta = 1,6$ are possibly made by trigger algorithm.

Bibliography

- [1] ATLAS Collaboration, Expected Performance of the ATLAS Experiment, Detector, Trigger and Physics, CERN-OPEN-2008-020, Geneva, 2008,
- [2] Andrea Di Simone, Diploma thesis, RPCs as trigger detector for the ATLAS experiment, University
- [3] F. Caradini; MUON-INT-2007-002
- [4] S. Borroni; ATL-PHYS-PROC-2009-102
- [5] M.Schott; ATL-PHYS-PROC-2009-039
- [6] M. Marcisovsky
- [7] http://en.wikipedia.org/wiki/Particle_physics.
- [8] The ATLAS Collaboration, G. Aad et al., 2008 JINST 3 S08003